

03

## Propagation of solitary pressure wave through the microwave discharge region in the air at medium pressures

© V.L. Bychkov,<sup>1</sup> L.P. Grachev,<sup>2</sup> I.I. Esakov,<sup>3</sup> A.V. Semenov<sup>3</sup>

<sup>1</sup> Moscow State University by M.V. Lomonosov,  
119991 Moscow, Russia

<sup>2</sup> Moscow Radio Technical Institute, Russian Academy of Sciences,  
117519 Moscow, Russia

<sup>3</sup> Vite Moscow University,  
115432 Moscow, Russia  
e-mail: iesakov@yandex.ru

Received March 4, 2021

Revised May 15, 2021

Accepted May 15, 2021

Results of experiments on a propagation of a pressure wave with a shock-wave leading front through a gas region excited by a pulsed freely localized discharge of the microwave wavelength range are described. The discharge was realized in air at a pressure from 14 to 100 Torr in the focal region of a quasi-optical electromagnetic beam of the microwave wavelength range. The experiments revealed three types of interaction of the gas-dynamic pulse with the region excited by the discharge in the post-discharge mode. The specific type of interaction is defined by the initial structure of the discharge and the delay time of the gas-dynamic pulse passage through the excited region.

**Keywords:** aerodynamics, microwave discharge, pressure wave.

DOI: 10.21883/TP.2022.14.55215.52-21

### Introduction

For reduction of the resistance at supersonic velocities two main physical effects are known, related to additional heat supply to the flow field. The first effect involves density reduction in the frontal area of the aerodynamic body (due to temperature rise), this implies using of constant heating. The other mechanism is a combination of low-density effects in the wake behind the heating zone and the flow field around the body, this can result in the creation of a completely different flow field. The magnitude of the effect on the flow field is different for different aerodynamic shapes of the aerodynamic body.

Plasma introduction into high-speed aerodynamic flow fields with their inherent strong gradients of physical parameters leads to the occurrence of many physical processes including complex interactions taking place during the passage of the shock wave (SW) [1,2]. Plasma is produced by means of various types of electrical discharges. Streamer (filamentous) discharges were investigated in order to find the methods of reducing air resistance at supersonic and hypersonic speeds. Those discharges can be very heterogeneous, both in space and time. They are often produced through high-frequency discharges and UHF (microwave) discharges. The greatest attention of researchers in terms of efficiency of the impact on the flows is drawn to microwave discharge [2,3]. This is primarily related to its high energy efficiency. Almost all microwave source energy, apart from that reflected from the discharge region and dissipated, is

consumed by such discharge at pressures above 30 Torr. Formation of a quasi-optical focused microwave beam allows igniting a pulsed gas electric discharge [2–6] in its focal area distant from the surrounding elements. Energy exposure to pulsed microwave discharge and laser radiation has generated considerable interest over the past few decades as a promising technique to control the flows at high and ultrahigh speeds [1,2].

Successful experiments in this area of research have been performed [7–13].

Thus, groups of researchers working with Kolesnichenko, Lashkov and Mashek [3,4] performed several experiments to study the effect of microwave plasma on the blunt cylinder resistance at Mach number 1.7 in a free stream flow at static pressure  $p_\infty = 8$  kPa and static temperature  $T_\infty = 200$  K. The microwave pulse was produced by a klystron operating at 9 GHz with peak power of 210 kW and pulse duration  $\tau = 1.2$  to  $2.2 \mu\text{s}$ . The discharge produced several plasmoids upstream of the blunt cylinder.

To study the characteristics of the occurring plasma, Exton [5] group performed an experiment to investigate the interaction of microwave plasma with a blunt cylinder at Mach number  $M = 6$  in a free-stream flow at static pressure  $p_\infty = 0.4$  kPa and static temperature  $T_\infty = 70$  K. The microwave pulse was produced by a klystron (at 15.8–17.3 GHz) with a peak power of 425 kW and pulse duration  $\tau \leq 3.5 \mu\text{s}$ .

The Lashkov–Mashek group [4] performed experiments to evaluate the interaction of the microwave discharge

on blunt and hemispherical cylinders at Mach number  $M = 2.1$  in the air in a free-stream flow at static pressure  $p_\infty = 3.3$  kPa and static temperature  $T_\infty = 159$  K. Subsequent experiments were carried out in many works by this team [7,8].

The experiments demonstrated a significant influence of the microwave discharge plasma on the parameters of the free-stream flow, and the optimal conditions for applications are investigated in new works [9–15].

In experiments, for discharge ignition at low gas pressures hermetic working chambers are used. In this case, the control radiations should be made to go out of the chamber through optically transparent portholes. This causes difficulties with interpreting the measurement results. Acoustic measurements can be taken by way of passing a gas-dynamic perturbation (GP) with a shockwave (SW) front edge through the discharge region. This article is devoted to the description of such experiments and their results. The present work is a sequel to similar studies described in [2,6]. The completed experiments clearly showed that depending on the initial type of the electrodeless freely localized pulsed discharge and the delay time from its end to the moment of probing after the GP discharge region, there exist three types of this region influence on the probing pulse parameters.

## 1. Experimental conditions

The experiments were performed on the installation which scheme is shown in Fig. 1.

A horizontal air-tight cylindrical working chamber, 60 cm in diameter and 160 cm long [2,6] was used in the experiments. Its inner side surface is covered with foam rubber. The pressure of ambient air in chamber  $p$  could be set within the range from 10 Torr to the atmospheric value, at minimum intervals of 1.5 Torr.

A linearly polarized electromagnetic (EM) wave with the wavelength  $\lambda = 8.9$  cm can be radiated into the working chamber as a quasi-optical beam of electromagnetic radiation (ER) through the radio-transparent end of that

chamber. The ER is focused on the camera axis in its central area. The experiments used single EM pulses with the length  $\tau_{pul} = 40 \mu\text{s}$ . The power of the ER beam in different pulses could be set within the range from  $P_{\min} \approx 10$  kW to  $P_{\max} = 500$  kW. In the focal plane, the ER beam had a Gaussian transverse distribution of the electric component amplitude of the EM wave  $E$ :  $E = E_0 \exp(-x^2/a^2)$  at  $a = 5.2$  cm in the vertical direction, and  $E = E_0 \exp(-y^2/b^2)$  at  $b = 2.5$  cm in the horizontal direction. The length of the ER beam focal region in the axial direction, with the field level  $E \gtrsim 0.8E_0$ , has the size of  $z_0 \approx 8$  cm. According to the formula [2–4]  $P = [E_0^2/(2Z_0)](\pi ab/2)$  where  $Z_0 = 120\pi$  is the wave impedance of free space. With  $P_{\min}$  the field is equal to  $E_0 = 600$  V/cm, while at  $P_{\max}$  the field size makes  $E_0 = 4$  kV/cm.

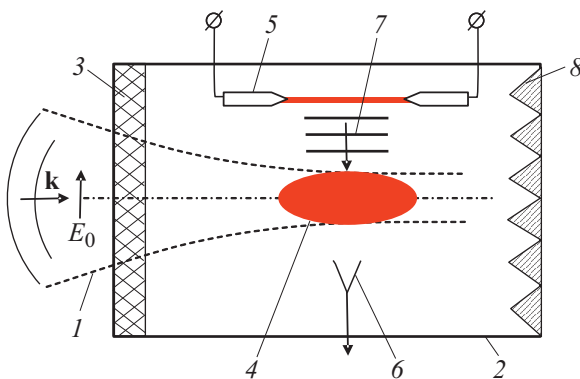
To ignite a discharge in an EM field, the level of its electric component  $E_0$  should be above the minimum — critical breakdown field  $E_{cr}$  at a given gas pressure  $p$ . For microwave air breakdown, field  $E_{cr} = 42p$ , [V/cm] [2,4] with [Torr] measuring unit for  $p$ , like in all similar formulas. This formula takes into account that in the experiments, at experimental value of  $\lambda$  corresponding to circular frequency  $\omega = 2 \cdot 10^{10}$  1/s, the resulting discharge plasma will be collisional, i.e., in it  $v_c > \omega$ , where the collision frequency of plasma discharge electrons with air molecules is  $v_c = 4 \cdot 10^9 \cdot p$ , [1/s] [2,4].

In the experimental variation range  $E_0$ , with due account for the formula for  $E_{cr}$ , the air can be broken within the pressure range  $p$  from 14 to 100 Torr. In this range, a freely localized supercritical microwave discharge will ignite in a diffuse or streamer form [2]. The boundary between those types of discharge  $E_{thres}(p)$  is quite sharp and at field  $E_0$  close to  $E_{cr}$ , falls within the range of  $p = (35–40)$  Torr. In our experiments, dependence  $E_{thres}(p)$  was experimentally specified. The results of those experiments are shown in Fig. 2.

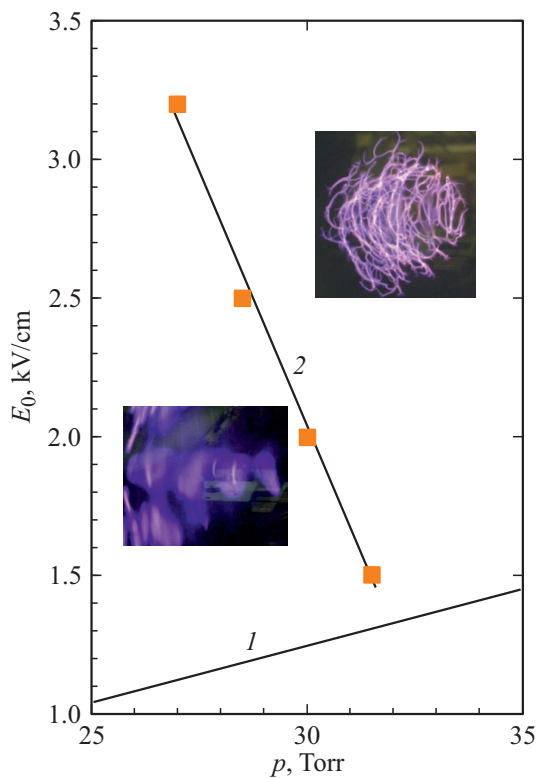
In the experiments, as shown in Fig. 1, the gas-dynamic perturbation probing the discharge region is produced by a pulsed linear gas discharge. Naturally, the energy of the produced gas perturbation increases with the growth of air pressure  $p$ . It follows from Fig. 2 that in the experiments at  $p = 30$  Torr, the type of discharge will change following the variation of field  $E_0 \geq E_{cr}$ . Thus, at  $E_0 \geq 1.3$  kV/cm to  $E_0 = 2$  kV/cm, it will be produced in diffuse form, while at  $E_0 > 2$  kV/cm — in streamer form.

Fig. 2 shows the pictures of a discharge in air at  $p = 30$  Torr in the focal region of the microwave beam in diffuse and streamer forms.

It follows from the experimental pictures analysis that the horizontal length scale of the discharge regions is  $z_{dis} \approx 10$  cm. Exactly that scale set the inter-electrode distance of the discharge arrester generating the cylindrical probing GP,  $z = 8$  cm. A capacitor with a capacity of  $C = 1 \mu\text{F}$ , precharged to  $U = 15$  kV, can be connected to the electrodes of this discharge arrester, through an appropriate switch. At this value of  $U$  and with the working chamber



**Figure 1.** Scheme of the experiment: 1 — ER beam, 2 — air-tight working chamber, 3 — radio-transparent window, 4 — discharge area, 5 — discharger — acoustic perturbation generator, 6 — acoustic wave receiver, 7 — probing UW, 8 — ER absorber.



**Figure 2.** The boundary between diffuse and streamer types of supercritical microwave discharge: 1 —  $E_{cr}(p)$ , 2 — experiment

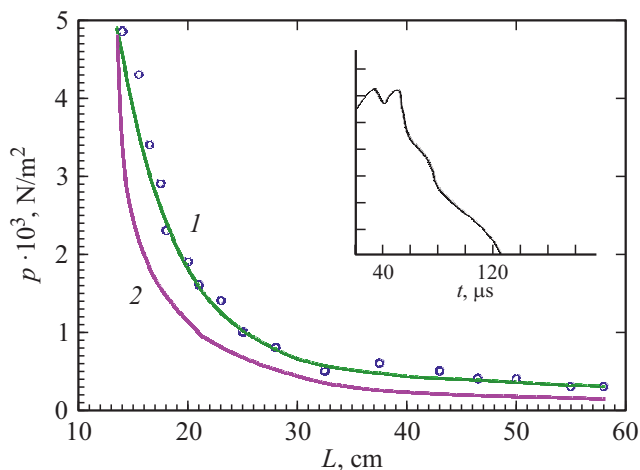


**Figure 3.** Dependence of overpressure at the GP front as measured along its trajectory: 1 — experiment, 2 — theory.

pressure of  $p = 30$  Torr, a linear pulse discharge lights up between the electrodes every time when the switch closes. That discharge is the source of the probing GP.

In the experiments, the receiver of that pulse is mounted in a line perpendicular to the axis of that discharge, at a distance  $L = 56$  cm, symmetrically to the electrodes. It is based on a barium titanate piezoelectric transducer, 5 mm in diameter and 0.6 mm thick. The attachment of the piezo-sensor allows almost complete damping of its self-

oscillations. The measuring circuit records pressure drops with a minimum duration of  $1 \mu\text{s}$  and tracks, almost with no distortion, its smooth changes with characteristic millisecond scale time intervals. The time between successive breakdowns of this arrester in the experiments was no less than 1 min.

Fig. 3 shows an experimental curve of overpressure measurements at the gas-dynamic perturbation front along its trajectory, without ignition of the discharge. It also shows the calculated dependence as determined on the basis of the relations specified in [2] for the initial triangular wave profile. You can see their relative match.

Fig. 3 also shows a characteristic oscilloscope record of the probing signal. Its horizontal scale is  $20 \mu\text{s}/\text{div}$ . The vertical scale is arbitrary. It is proportional to the overpressure. It follows from the oscilloscope record that the probing perturbation has a shock front edge.

## 2. Results of the main experiments

The main experiments were carried out at the chamber pressure  $p = 30$  Torr. In those experiments, the field  $E_0$  and the delay time of the probing GP varied, with respect to the moment of switching on field  $t_{delay}$ .

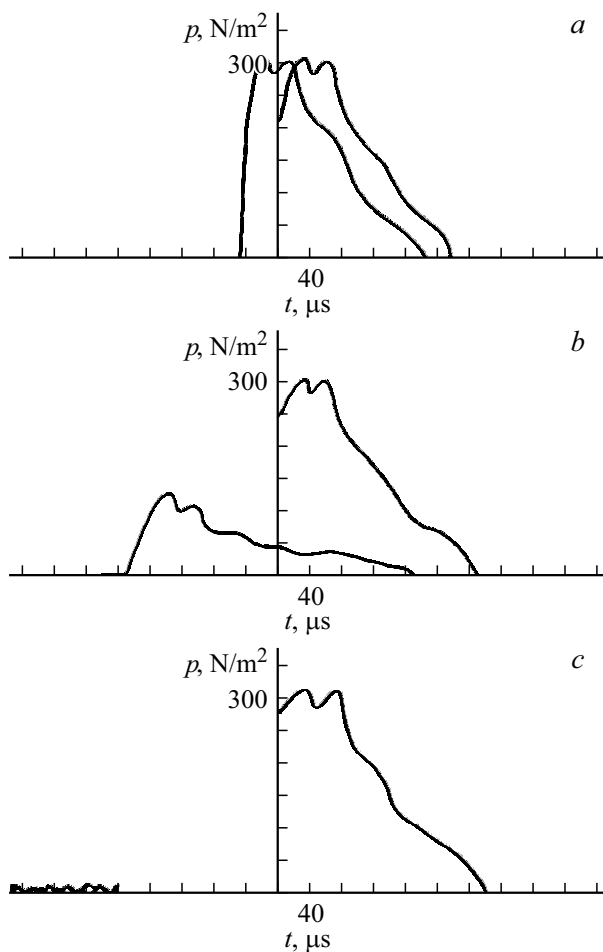
Fig. 4 shows a set of oscilloscope records corresponding to field  $E_0 = 2.2 \text{ kV/cm}$ , i.e., to the streamer discharge. The oscilloscope records on the right-hand side are the results of control experiments, i.e. they were produced in the absence of a discharge, while the left-hand side ones were produced with the inclusion of the discharge and at different time  $t_{delay}$ .

Fig. 4, *a* corresponds to a relatively long delay time  $t_{delay} = 0.2$  s. In this case, the first type of interaction is implemented of the control SW with the post-discharge region of the discharge. It follows from the figure that the probing pulse reaches the receiver faster, while its amplitude and shape remain practically the same. That type of interaction in the experiments at given  $p$  and  $E_0$  was recorded for the entire delay time  $t_{delay} > 8 \cdot 10^{-2}$  s.

At shorter time  $t_{delay}$  within the range from  $5 \cdot 10^{-3}$  to  $8 \cdot 10^{-2}$  s, the second type of interaction is implemented of the control gas-dynamic pulse with the post-discharge region of the discharge. Its respective oscilloscope record is shown in Fig. 4, *b*. It follows from those records that in such type of interaction the probing pulse reaches the receiver faster, its amplitude reduces significantly and the front edge becomes slanted. The area of the recorded pulse also reduces compared to the reference one.

Finally, at an even shorter time  $t_{delay}$  the third type of interaction illustrated in Fig. 4, *c*, is implemented. In that case the structure of the probing gas-dynamic pulse collapses.

We pointed out that field  $E_0$  varied in the experiments and both streamer and diffuse forms of discharge could be realized. In this case, only the first and second types of interaction of the control GP with the discharge region



**Figure 4.** Types of weak SW interaction with the electrodeless discharge plasma

were recorded in the experiments over the entire range of the diffuse form realization. And even at  $t_{delay} = 0$  the control GP passed through the discharge region changing its characteristics in accordance with Fig. 4, *b*, without full destruction.

Thus, the experiments identified three types of interaction between the pulsed gas perturbation and the shock front as it passes through the discharge region.

### Conflict of interest

The authors declare that they have no conflict of interest.

### References

- [1] V.L. Bychkov, L.P. Grachev, I.I. Yesakov, A.V. Semenov. *ZTF*, **90** (8), 1283 (2020). (in Russian)
- [2] L.P. Grachev, I.I. Yesakov, K.V. Aleksandrov, A.A. Ravaev, L.G. Severinov, K.V. Khodataev. *Gazovy Elektricheskiy Razryad v Kvaziopticheskom SVC-puchke* (AO „MRTI RAN“, M., 2015) (in Russian)
- [3] *Trudy Instituta Obschey Fiziki RAN* (in Russian) *Fizika i Khimiya Gazovykh Razryadov v Puchkakh SVC -Voln* (Nauka, M., 1994), t. 47. (in Russian)
- [4] *Vysokochastotny Razryad v Volnovykh Polyakh*, pod red. A.G. Litvak V sb. nauch. tr. (in Russian) IPF AN SSSR (IPF AN SSSR, Gorkiy, 1988) (in Russian)
- [5] A.S. Zarin, A.A. Kuzovnikov, V.M. Shibkov. *Svobodno Lokalizovanny SVC-Razryad v Vozdukh* (Neft i Gaz, M., 1996) (in Russian)
- [6] L.P. Grachev, I.I. Yesakov, G.I. Mishin, M.Y. Nikitin, K.V. Khodataev. *ZTF*, **55** (5), 972 (1985). (in Russian)
- [7] V. Fomin, P. Tretyakov, J.-P. Taran. *Aerospace Sci. Technol.*, (8), 411 (2004).
- [8] D.J. Knight. *Propulsion Power.*, **24** (6), 1153 (2008).
- [9] Y. Kolesnichenko, V. Brovkin, S. Leonov, A. Krylov, V. Lashkov, I. Mashek, A. Gorynya, M. Ryvkin. *AIAA Paper* 2001–0345 (2001).
- [10] V. Lashkov, I. Mashek, Y. Anisimov, V. Ivanov, Y. Kolesnichenko, M. Ryvkin, A. Gorynya. *AIAA Paper* 2004–0671 (2004).
- [14] R. Exton, R. Balla, B. Shirinzadeh, G. Herring, J. Fugitt, C. Lazard, K. Khodataev. *Phys. Plasmas*, **8** (11), 5013 (2001).
- [12] V.A. Lashkov, A.G. Karpenko, R.S. Khoronzhuk, I.Ch. Mashek. *Phys. Plasmas*, **23**, 052305 (2016). <https://doi.org/10.1063/1.4949524>
- [13] A.I. Saifutdinov, E.V. Kustova, A.G. Karpenko, V.A. Lashkov. *Plasma Phys. Rep.*, **45**, 602 (2019). <https://doi.org/10.1134/S1063780X19050106>
- [14] V.G. Brovkin, P.V. Vedenin. *J. Appl. Phys.*, **128**, 113301 (2020). DOI: 10.1063/5.0016249
- [15] A.I. Saifutdinov, E.V. Kustova. *J. Appl. Phys.*, **129**, 023301 (2021). <https://doi.org/10.1063/5.0031020>